

# Comprehensive thermal preference phenotyping in mice using a novel automated circular gradient assay<sup>†</sup>

Filip Touska<sup>a,b,‡</sup>, Zoltán Winter<sup>a,‡</sup>, Alexander Mueller<sup>a</sup>, Viktorie Vlachova<sup>b</sup>, Jonas Larsen<sup>c</sup>, and Katharina Zimmermann<sup>a</sup>

<sup>a</sup>Klinik für Anästhesiologie am Universitätsklinikum Erlangen, Friedrich-Alexander Universität Erlangen-Nürnberg, Erlangen, Germany;

<sup>b</sup>Department of Cellular Neurophysiology, Institute of Physiology of the Czech Academy of Sciences, Prague, Czech Republic; <sup>c</sup>Independent scholar, Erlangen, Germany

## ABSTRACT

Currently available behavioral assays to quantify normal cold sensitivity, cold hypersensitivity and cold hyperalgesia in mice have sometimes created conflicting results in the literature. Some only capture a limited spectrum of thermal experiences, others are prone to experimenter bias or are not sensitive enough to detect the contribution of ion channels to cold sensing because in mice smaller alterations in cold nociception do not manifest as frank behavioral changes. To overcome current limitations we have designed a novel device that is automated, provides a high degree of freedom, i.e. thermal choice, and eliminates experimenter bias. The device represents a thermal gradient assay designed as a circular running track. It allows discerning exploratory behavior from thermal selection behavior and provides increased accuracy by providing measured values in duplicate and by removing edge artifacts. Our custom-designed automated offline analysis by a blob detection algorithm is devoid of movement artifacts, removes light reflection artifacts and provides an internal quality control parameter which we validated. The assay delivers discrete information on a large range of parameters extracted from the occupancy of thermally defined zones such as preference temperature and skew of the distribution. We demonstrate that the assay allows increasingly accurate phenotyping of thermal sensitivity in transgenic mice by disclosing yet unrecognized details on the phenotypes of TRPM8-, TRPA1- and TRPM8/A1-deficient mice.

## ARTICLE HISTORY

Submitted 10 November

2015

Revised 15 December 2015

Accepted 15 December 2015

## KEYWORDS

nociception; skew; thermal selection; thermosensation; TRPM8; TRPA1

## Introduction

Temperature perception, thermoregulation and thermoregulatory behavior are evolutionary important sensory abilities and exist in all living organisms. In recent years the cellular and molecular mechanisms of temperature sensing and thermoregulation were subject of intensive research and have led to the generation of insightful transgenic mouse models that lack specific proteins and ion channels, such as members of the TRP ion channel group that function as molecular thermometers in sensory neurons for environmental temperatures from noxious hot to noxious cold.<sup>1,2</sup> A major breakthrough for the molecular understanding of cold sensing was the identification of the “cold and menthol” receptor TRPM8,<sup>3,4</sup> because characterization of

TRPM8-deficient mice revealed broad cold-sensing deficits albeit not a complete lack of cold avoidance.<sup>5–7</sup> TRPA1 was discovered as a cold transduction channel with activation in the noxious temperature range, and as sensor for pungent compounds, environmental irritants and mediators of inflammatory pain.<sup>8–10</sup> Nevertheless, cold sensitivity of the TRPA1 receptor and its contribution to cold avoidance in mice was a matter of debate for a long time, but very recently TRPA1 cold sensitivity was demonstrated to be an inherent property of the molecule when the purified and reconstituted channel was examined in lipid bilayers.<sup>11</sup> Yet the current evidence still does not consolidate a unifying view to which extent TRPA1 contributes to cold sensing *in vivo*. Also because mice lacking

**CONTACT** Katharina Zimmermann  [katharina.zimmermann@fau.de](mailto:katharina.zimmermann@fau.de)  Klinik für Anästhesiologie am Universitätsklinikum Erlangen, Friedrich-Alexander Universität Erlangen-Nürnberg, Krankenhausstraße 12, 91054, Erlangen, Germany.

Color versions of one or more of the figures in the article can be found online at [www.tandfonline.com/ktmp](http://www.tandfonline.com/ktmp).

<sup>†</sup>This article was submitted through the Accelerated Track.

<sup>‡</sup>These authors contributed equally to this work.

© 2016 Filip Touska, Zoltán Winter, Viktorie Vlachova, Jonas Larsen, and Katharina Zimmermann. Published with license by Taylor & Francis.

This is an Open Access article distributed under the terms of the Creative Commons Attribution-Non-Commercial License (<http://creativecommons.org/licenses/by-nc/3.0/>), which permits unrestricted non-commercial use, distribution, and reproduction in any medium, provided the original work is properly cited. The moral rights of the named author(s) have been asserted.

TRPM8 and TRPA1 were shown to have no additional deficits in cold avoidance in a 2-temperature choice assay during a 5 minute testing period, which was so far the only cold avoidance test they were subjected to.<sup>12</sup> In living animals TRPA1 has been shown to be relevant for cold hypersensitivity in pathophysiological conditions in the presence of proinflammatory mediators.<sup>13,14</sup> In addition TRPA1<sup>-/-</sup> mice exhibit avoidance deficits in the noxious cold range, when challenged at temperatures close to 0°C on a cold plate assessed in a 5 minute period and a reduction in paw lifting and shaking duration after acetone cooling<sup>15</sup>; another study confirmed these findings also by showing less nocifensive behavior, reduced number of jumps on a cold plate (0°C) in a 2 minute period and an increased flicking latency upon tail immersion in a -10°C water-methanol mixture.<sup>16</sup> In contrast, TRPA1<sup>-/-</sup> didn't exhibit any alteration in temperature preference measured with a 2-temperature choice assay (0–30°C).<sup>6,17</sup> Nevertheless our recent study of an assessment of the brain processing of a 15°C cold temperature stimulus by fMRI in TRPA1-deficient mice revealed a contribution of TRPA1 to cold perception at higher temperatures than estimated earlier. Although this study brought evidence that TRPA1-carrying fibers are activated at much higher temperatures than previously thought, the resulting alterations in perception are seemingly too small to lead to overt changes in the commonly used mouse behavioral assays.<sup>18</sup>

These findings and conclusions highlight the difficulties limiting comprehensive phenotyping of murine temperature sensing and thermal selection behavior and the need to examine mouse behavior over longer periods of time and in more complex experimental environments than a 2-plate choice assay provides. Furthermore, the rising number of potential candidate proteins involved in thermosensitivity<sup>1</sup> increase the need for accurate characterization of thermal selection behavior under precisely defined experimental conditions because the key evidence sought after when targeting specific proteins in murine molecular pathways is the identification of a behavioral phenotype leading to the recognition of the protein's function in thermosensory systems. Here we introduce an improved thermal gradient assay design that enables more precise, automated and bias-free assessment of murine thermal preference.

In fact, temperature gradient assays are not novel; they were first introduced for studies of autonomic and behavioral thermoregulatory responses. Designs of plexiglas tubes with surrounding copper coils of variable spacing allowing the control of ambient temperature in the tube were used first<sup>19,20</sup>; and, more complex constructions allowed to house animals in the gradient for 24h periods with simultaneous assessment of core temperature.<sup>21</sup> Later constructions were built to generate conductive floor temperature gradients to measure the preferred foot pad temperature in mice. They contained slots in the floor to prevent convective temperature gradients.<sup>22,23</sup> Our new design is derived from the conductive floor temperature gradient first introduced and used by Gordon.<sup>22</sup> However, in contrast to Gordon's linear design, which was also employed by Dhaka to phenotype thermal preference in TRPM8-deficient mice,<sup>7</sup> we constructed a circular running track to eliminate border bias with the advantage of duplicate data points for each virtual temperature zone and superior options for data analysis. To validate the new design, we put the phenotypes of common knockout mouse strains lacking the cold transducer ion channels TRPA1 and TRPM8 and the double knockout mice to the test. Our results shed more light on the cold sensing phenotypes of these transgenic mice and contribute to the highly discussed and partially controversial science of cold sensing.

## Materials and methods

### Thermal gradient apparatus

Our circular assay was assembled in 2 configurations, small and large. Both configurations consist of a ring-shaped 1.5 cm thick aluminum disk that provides a circular running track for the mouse to move freely. The dimensions of inner and outer ring diameter are 28 cm and 40 cm for the smaller, and 45 cm and 57 cm for the larger assembly. Inner walls of plexiglas and outer walls of aluminum, both of 12 cm height with circumferences of 88 and 126 cm or 141 and 179 cm, respectively, confine a circular surface area of 640 cm<sup>2</sup> or 960 cm<sup>2</sup>, respectively, with a width of 6 cm on which a temperature gradient is equilibrated. The surface is stained in frosted orange (eloxadized aluminum with minimal light reflection) to provide sufficient contrast for mouse detection, but also to allow

surface temperature control with an infrared camera. During measurements the running track is uniformly illuminated and the mouse behavior is videotaped with a regular CCD camera. The outer walls are made non-transparent to mask positional cues.

The thermal gradient is constantly equilibrated across the aluminum disk using 2 feed-back controlled peltier-based plates (TE Technology, Traverse City, MI, USA) in combination with a custom-built temperature controller (Labortechnik Franken, Röthenbach, Germany). To optimize thermal conductivity, the peltier plates are lubricated with a thin layer of thermoconductive paste and opposite sides of the aluminum ring are screwed tightly onto the plates. The stability of the surface temperature gradient is monitored before each measurement with an infrared camera (T400 series, FLIR(R) Systems GmbH, Frankfurt, Germany). Deviations of less than  $\pm 1$  °C were tolerated, but readjusted.

A transparent lid is labeled to divide the small ring in 15 and the large ring in 22 even-sized and one larger zone. Each individual zone covers a surface area of 40 cm<sup>2</sup> while the one larger zone covers 80 cm<sup>2</sup> and marks the coldest area. It is required for unambiguous offline analysis of videotaped behavior with a custom-engineered software which is described below. The symmetric assembly yields 2 semi-circles of even temperature on opposite sides. Consequently, for each thermal zone measured values are provided in duplicate and values of each 2 zones of equal temperature are added; in our assemblies 8 and 12 zones resulted (Fig. 1).

### Automated data analysis: Software detection algorithm

A software algorithm was written by JL for offline video analysis. The software consists of a python/Tkinter-based graphical user interface (GUI) and a backend which is implemented in C++. The algorithm detects the position of one mouse in a circular device, using computer vision. The mouse position is detected from frame-by-frame analysis and thus does not rely on movements (differential changes between movie frames). Initially, a background image is computed by considering the pixel-by-pixel intensity variations over time. The movie is split into frames (we used 1 frame per second), and the mouse position is detected by analyzing the center of mass of the residual between each frame and the background. The geometry of the rings and zones is detected (using Canny

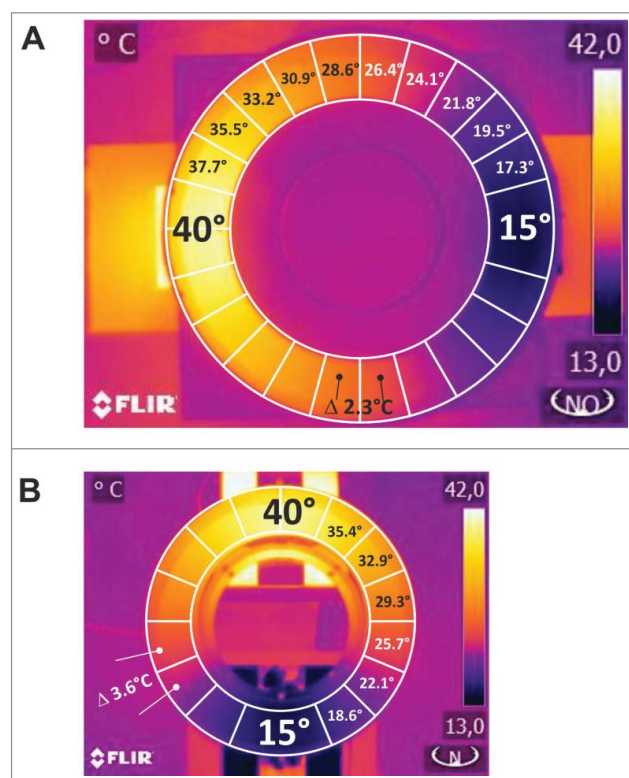


**Figure 1.** Illustration of the assay design. (A, B) Infrared photographs with overlaid schematic illustrations of (A) 12 and (B) 8 zone temperature preference assays: top view of the ring-shaped disc, supplemented with inner and outer boundary where one mouse can move freely. The ring is divided into 22 (A) or 14 (B) even-sized plus one large zone. The zone boundaries are marked on the transparent plexiglas lid. The disk is heated and cooled on opposite sides to establish a continuous temperature gradient. The gradient is symmetric and for data analysis each 2 zones of even temperature on opposite sides are summarized to yield 8 or 12 zone histograms. Mouse behavior is recorded during 60 min using a CCD-camera. Custom-designed software performed the analysis and extracted location of the mouse with respect to the indicated zones in the desired time resolution. In both designs, individual zones have the same size, which results in a gradient of (A) 2.27°C (0.31°C/cm) or (B) 3.57°C (0.47°C/cm). Dimensions of each assay are outlined in methods.

edge detection and Hough transforms), and the mouse is assigned to a zone in each frame. The result of the analysis is reported, 1) as the original movie with additional indications of the detection of the mouse and, 2) as a .csv indicating the distribution of zones over time and the number of times that the mouse entered any zone.

### Animal models

#### Transgenic mice

We used adult naïve TRPM8<sup>-/-</sup> (Dhaka et al., 2007) which were backcrossed for 5 generation on C57BL/6J

background, and TRPA1<sup>-/-</sup> (Kwan et al., 2006), backcrossed on 13 generations on C57BL/6J mice. From both we crossed and bred TRPM8/A1<sup>-/-</sup>M8<sup>-/-</sup>; we used a common age- and sex-matched control group. C57BL/6J mice for breedings were purchased from Charles River (Sulzfeld, Germany) and are genetically identical to C57BL/6J from the Jackson Laboratories (Bar Harbor, Maine, USA). All mice were between 60–85 d, Transgenic mice were genotyped according to our previously published procedures.<sup>18,24</sup>

### Behavioral measurements

All mice were subjected to acclimation for 30 mins with the aluminum floor of the device acclimatized to room temperature (22–24°C). On the day of the experiment, mice were measured in the apparatus at 15°–40°C and the room temperature set to 27°C. The individual who placed the mice in the behavioral apparatus was aware of mouse genotype, but all behavioral data were videotaped with the operator absent from the room.

### Statistics

For statistical analysis between 2 groups the t-test, for more than 2 groups ANOVA 'planned comparison' with Fisher LSD posthoc test was computed using Statistica version 7.1 (Dell Inc., Round Rock, TX, USA; formerly StatSoft, Tulsa OK, USA). Differences were considered significant at  $P < 0.05$  and are marked by asterisks in figures. Error bars in figures are displayed as SEM or SD, as indicated in legends.

## Results

### Validation of the software

To ease data mining, we first extracted a parameter from the software that allows us to validate how accurately the software measures the location of the mouse within the circular device. This parameter describes for each cropped frame the fidelity of blob detection as the ratio  $\geq 1$  between the most intensive and second-most intensive peaks in the residual image. The value is written onto each frame. It can be reviewed in the movie and as continuous data set ranked from lowest to highest ratio in a separate .csv file. We validated the hypothesis that low values signify increasing likelihood of erroneous detections. As a QC parameter for analyzed movies we chose the 1st percentile of the ratio value over all frames of one movie. Validation

of the QC-parameter was performed manually by reviewing 80 randomly taken movies under variable light conditions (282600 frames). For validation we selected movies mostly with 1st percentile values between 1 and 2, and especially 1.1. On every frame the most intensive peak is marked with a red spot and the second most intensive peak with a blue spot. To yield a true value, the mouse must be marked with the red spot, and then the labeled zone corresponds to the location of the mouse. If the mouse was labeled with the blue spot or not labeled, the detection was erroneous. In 282600 frames 6130 values were erroneous. Figure 2 A illustrates for each ratio between 1 and 15 the percentage of true detections and shows the number of frames analyzed per ratio. A ratio above 1.3 indicates that the mouse location was 90% correct; above 1.6 recognition fidelity exceeded 98%. Figure 2 B illustrates how this statistic relates to the 1st percentile value of a whole movie with 1800 frames or 3600 frames. Movies with a 1st percentile value of higher than 1.07 had a very high likelihood of containing equal or less than 1% erroneous allocations. Nevertheless this does not exclude that occasionally outliers occur. Low ratios and erroneous detections were in most cases due to unfavourable shades produced by poor illumination uniformity of the ring. If this occurred in combination with the mouse lingering close to the inner edges, this entails that the mouse is partly obscured by the shadow tail and the ratio remains close to 1 because this combination decreased the contrast and herewith the blob size. 1st percentiles were in general above 2 when vertical and uniform illumination of the whole ring was maintained. Keeping these conditions after the validation process, we achieved 1st percentiles ranging between 1.33 and 6.25 (median 3.43) for all movies in our study; only 5 of the 100 movies recorded in the large assembly and illustrated in this study had a 1st percentile below 2. Movies recorded in the small assembly were manually checked for potential misallocations and contained less than 1% errors.

### Measurement parameters

Summary .csv data were imported in MS Excel for further analysis. In MS Excel the *Thermal zone occupancy* was calculated to indicate the percent time spent in each zone in minute resolution (zones as indicated in Fig. 1). These values were subjected to a 3 adjacent data point averaging procedure before statistical calculation and visualized as entire time course over 60 min (Fig. 3 and 4 panels C and D). This set of data allows calculating the

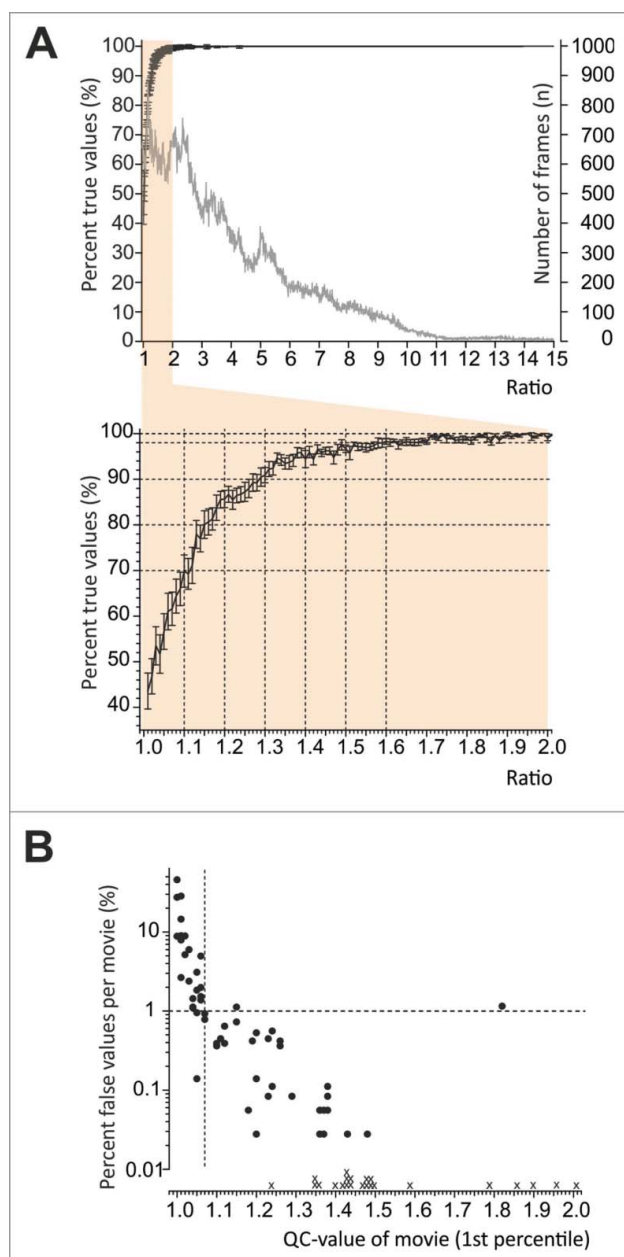


**Figure 2.** Validation of the software algorithm. Mouse behavior is videotaped and analyzed offline using custom-designed software. The fidelity of blob detection is described as the ratio  $\geq 1$  between the most intensive and second-most intensive peaks detected on each frame. (A) 282600 frames were verified manually to validate the ratio as parameter for quality assessment. Percent true detections for each ratio between 1 and 15 (black line, left Y-axis) and number of analyzed frames for each ratio are shown (gray line, right Y-axis). The inset expands ratios between 1 and 2 and illustrates that frames with ratios above 1.3 yielded  $>90\%$  true detections, for ratios above 1.6 recognition fidelity exceeded 98%. Error bars indicate SEM. (B) For each movie the 1st percentile was used as parameter to assess recognition fidelity and the figure illustrates how the statistic calculated in A relates to the 1st percentile value of an entire movie with 1800 frames or 3600 frames. Movies with a 1st percentile value of  $\geq 1.07$  had a high likelihood of containing equal or less than 1% misallocations. Nevertheless occasionally outliers occurred. "X" mark 1st percentiles of movies with 0% misallocations (not shown in log scale).

time lag in minutes after which mice do exclusively locate above a given temperature, such as  $27.5^{\circ}\text{C}$  (representing 50% surface in both assays) and  $31^{\circ}$  or  $32^{\circ}\text{C}$  (representing 37.5 or 33% surface in the small or large assay, respectively).

The *preference temperature* ( $\mu$ ) was calculated as the weighted average of occupied temperature using the following equation:  $\mu = \frac{\sum x_T T}{\sum x_T}$ , whereby  $x_T$  is the time spent in the zones with temperature  $T$ . The *standard deviation SD* ( $\sigma$ ), was calculated using the equation:  $\sigma = \sqrt{(\sum x_T T^2) - \mu^2}$  whereby  $\sum x_T T^2$  is the second moment. Preference temperature and its SD were calculated in minute resolution to yield a time course, but also averaged for every 15 min period to separate exploratory behavior from thermal selection behavior (Figs. 3 and 4, panel B; Tables 1 and 2). *Zone occupancy* was calculated as the percentage of time spent in each single zone and reproduced as histogram distribution per every quarter of an hour of observational time (compare Figs. 3 and 4, panel A).

For measurements in the large assay, as further measure for the distribution about the mean we calculated the third moment to describe the symmetry of the distribution, the *skew* ( $\gamma$ ). Skew was calculated as  $\gamma = \frac{E[T^3] - 3\mu\sigma^2 - \mu^3}{\sigma^3}$ ; with  $\sigma$  calculated for the population and the third moment  $E[T^3]$  calculated as  $\frac{\sum (x_T T^3)}{\sum x_T}$ . The  $\sigma^3$  factor makes skew a dimensionless number.

#### **No influence of slope of thermal gradient and surface area on thermal selection of C57BL/6 mice**

We were interested in evaluating temperature preference behavior within the innocuous temperature range. To compare the influence of gradient and surface area on preference behavior, we established a  $25^{\circ}\text{C}$  gradient from  $15^{\circ}$  to  $40^{\circ}\text{C}$  in the small and the large assembly. This results in a  $3.57^{\circ}\text{C}$  ( $0.47^{\circ}\text{C}/\text{cm}$ ) or a  $2.27^{\circ}\text{C}$  ( $0.31^{\circ}\text{C}/\text{cm}$ ) gradient between virtual adjacent fields in the small and the large assembly, respectively. Both assemblies are illustrated in Figure 1 A, B. We measured male naïve C57BL/6J mice ( $n = 14-20$ ) in both assemblies and found that the difference between the assay designs (thermal resolution, slope of the gradient, size of the assay) has no influence on exploratory behavior or on the preferred

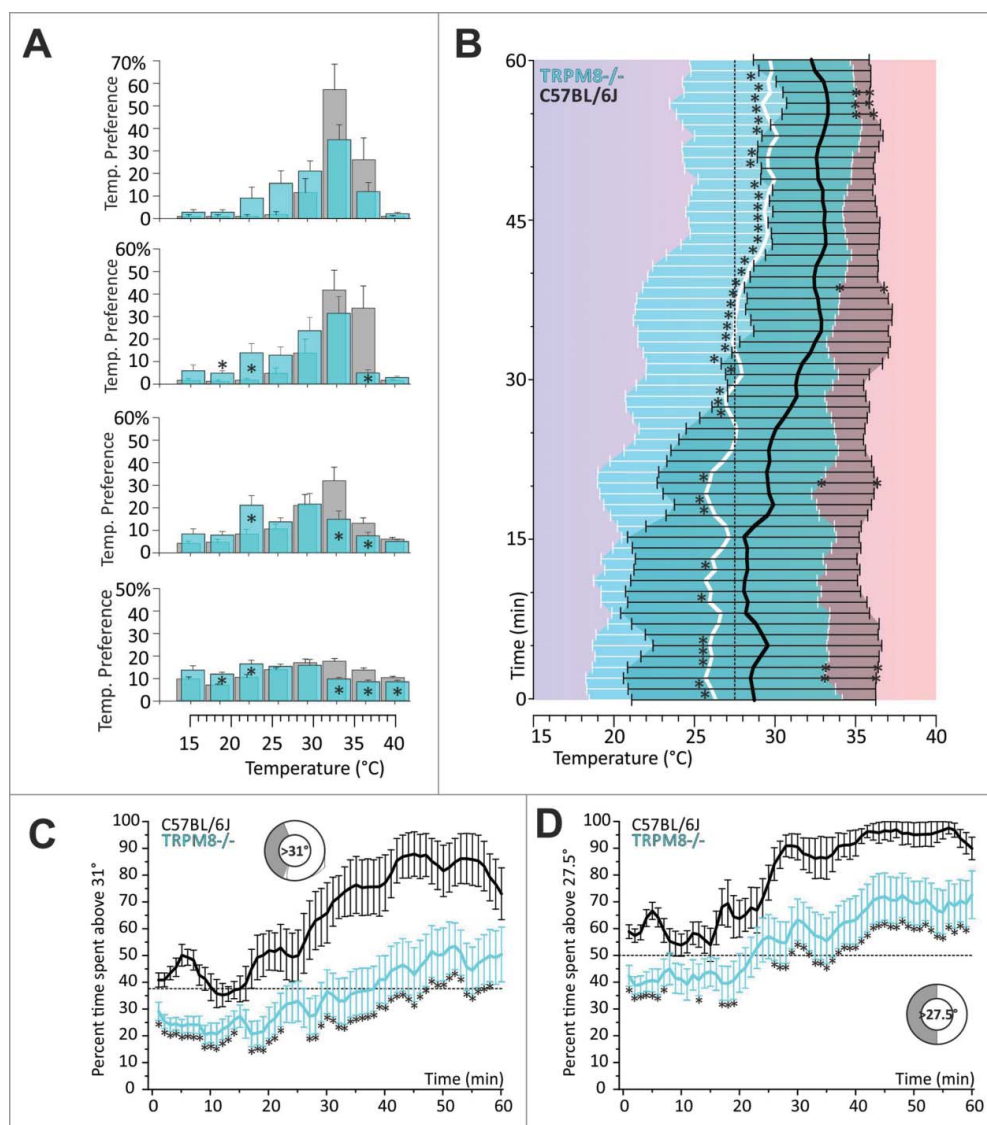


**Figure 3.** 8-zone assay: TRPM8-deficient mice show warm avoidance and reduced avoidance of innocuous cool. (A) Eight-zone histograms of zone preference of TRPM8<sup>-/-</sup>: (blue bars: TRPM8<sup>-/-</sup>; gray bars: C57BL/6J): from bottom to top, zone preference is summarized for each consecutive quarter of an hour as percent of time spent in each of 8 zones. Respective values of preference temperature, including standard deviation are indicated in the Table 1. Note: in mins 1–45: TRPM8<sup>-/-</sup> mice show both warm avoidance and reduced cold avoidance. Error bars are SEM. (B) Preference temperature time course from bottom (start) to top (60 min): throughout 60 mins thermal selection behavior of TRPM8<sup>-/-</sup> is significantly different from control. Over time TRPM8<sup>-/-</sup> mice migrate to warmer, but prefer markedly cooler floor temperature than control mice. At later time points mice progressively migrate to warmer floor temperature which also results in a reduction in SD. Data were subjected to a 3pt averaging procedure. Error bars with areas under the curve in cyan (TRPM8) and black (control) indicate SD and SD are significantly different for the asterisks on error bars. (C, D) Timecourses of temperature selection: percent time spent (C) above 31°C and, (D) in the warmer semicircle (above 27.5°C), calculated in 1 min resolution (average of 60 values per min) and subjected to a 3pt averaging procedure. Note: warm avoidance of TRPM8<sup>-/-</sup> is evident in the initial 20 mins in both panels. Error bars are SEM. Sketches illustrate temperature and respective fraction of floor surface; dotted black line illustrates the random probability to cover the respective part of the assay. Error bars indicate SEM. In all panels: colors: cyan: TRPM8<sup>-/-</sup> (n = 21), gray/black C57BL/6J (n = 14); asterisks refer to p < 0.05, T-test.

temperature to which the mice locate at the end of the observation time. In the small assembly this was 32.9° ± 2.4°C and 33.3° ± 3.1°C in the large one (Figs. 3 and 4, Tables 1 and 2); similarly, the time course of the temperature preference and the standard deviation were the same in both assemblies (Figs. 3 and 4).

#### Test time and surface area influence cold avoidance of TRPM8-deficient mice

TRPM8<sup>-/-</sup> mice have been subjected to a series of different behavioral tests, since their first publication in 2007 with the common result that TRPM8 is essential

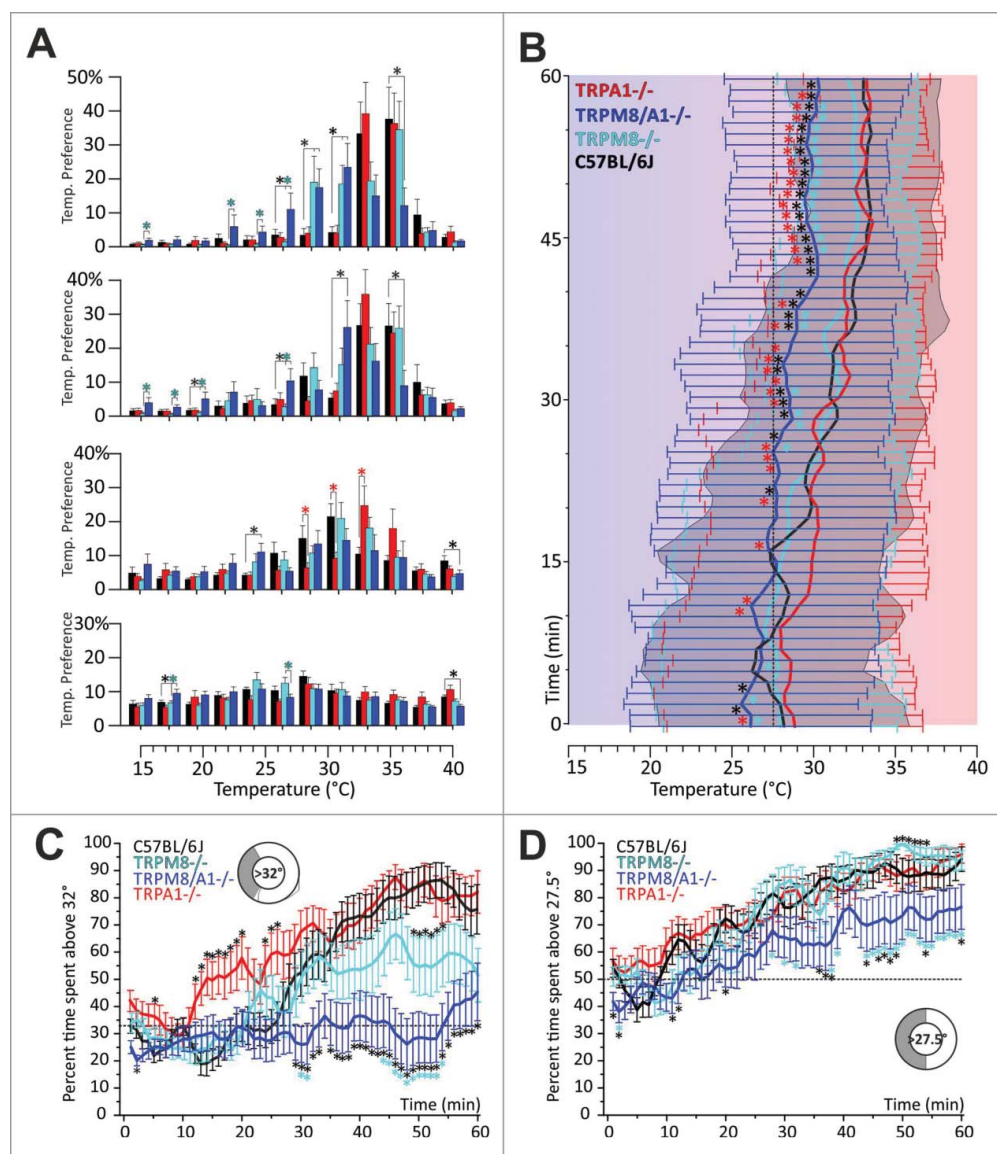


**Figure 4.** TRPM8<sup>-/-</sup>, TRPA1<sup>-/-</sup>, TRPM8/A1<sup>-/-</sup> strain comparison in the 12 zone-assay. (A) Histograms of zone preference of C57BL/6J (black), TRPA1<sup>-/-</sup> (red), TRPM8<sup>-/-</sup> (cyan) and TRPM8/A1<sup>-/-</sup> (blue): from bottom to top, zone preference is summarized for each consecutive quarter of an hour as percent of time spent in each of the 12 zones. Respective values of preference temperature per each 15 mins are indicated. After 30 min double knockout mice clearly select colder floor temperatures and show a broader tolerance for innocuous cool temperatures. TRPA1<sup>-/-</sup> mice have no deficits in cold avoidance but locate faster to warm surfaces. red asterisks: TRPA1<sup>-/-</sup> vs control; cyan asterisks: TRPM8 vs. TRPM8/A1<sup>-/-</sup>; black asterisks: knockout vs. control. Error bars are SEM. (B) Preference temperature time course from bottom (start) to top (60 min) in 4 genotypes: in the second half hour, thermal selection behavior of double knockout separates from TRPA1<sup>-/-</sup>, TRPM8<sup>-/-</sup> and controls. Double knockout mice still prefer warmer, but ~3°C colder floor temperatures than all other strains. Error bars represents SD; data were subjected to a 3pt averaging procedure; gray area: SD of control mice; all asterisks compare TRPM8/A1<sup>-/-</sup> to respective other strain indicated by color. Note that time courses of 8 and 12 zone assay in C57BL/6 controls are indifferent (compare to Fig. 3). (C, D) Time courses of temperature selection: percent time spent (C) above 32°C and, (D) in the warmer semicircle (above 27.5°C) calculated in 1 min resolution (averaging from 60 values per min) and subjected to a 3pt averaging procedure. Error bars are SEM. Sketches illustrate temperature and respective fraction of floor surface; dotted black line illustrates the random probability rate to cover the respective part of the assay. Note: TRPA1/M8<sup>-/-</sup> still prefer to migrate to the warmer semicircle in the second half of the experiment, but they only locate to about 30% above 32°C which is the random probability rate. In all panels: TRPM8<sup>-/-</sup> n = 19, TRPM8/A1<sup>-/-</sup> n = 20, TRPA1<sup>-/-</sup> n = 20, C57BL/6J n = 20; asterisks refer to p < 0.05, ANOVA with Fisher LSD PostHoc test.

for the detection of environmental cold. Mostly this conclusion results from studies with 2 temperature choice assays (based on 2-plate paradigms) but also

from a 100 cm long linear gradient assay adjusted between 15° and 53.5°C, providing a resolution of 0.39°C/cm<sup>7</sup>. Our large assay provides a length of 160/

2 cm and thereby a resolution of  $0.31^{\circ}\text{C}/\text{cm}$  per semicircle (calculated for the center of the ring  $\pm 0.028^{\circ}\text{C}$  for inner and outer limits) and the small one resolves  $0.47^{\circ}\text{C}/\text{cm}$  ( $\pm 0.04^{\circ}\text{C}$ ) in a middle circumference of 107 cm. In our assay, TRPM8-deficient mice displayed a prominent reduction in cold avoidance only in the smaller 8-zone assay, where they finally located to  $29.7^{\circ} \pm 3.5^{\circ}\text{C}$ , at  $3.2^{\circ}\text{C}$  colder temperatures than controls (Fig. 3, Table 1). In addition we found that TRPM8<sup>-/-</sup> display a marked avoidance of warmer zones which is most prominent during the first 45 min of exposure as seen from both the histogram view (Fig. 3A) and the timecourse of thermal selection for temperatures above  $31^{\circ}\text{C}$ , where the average time spent is lower than the random probability rate of 37.5% (Fig. 3C). In this assay it became also clear that TRPM8<sup>-/-</sup> still recognized warmer zones as preferable to colder areas, but required more time than controls to migrate there, potentially also because they feel repulsed by warm temperatures (Fig. 3B). While the controls spend from the beginning at least 50% of their time in the warmer semicircle (zones with temperatures higher than  $27.5^{\circ}\text{C}$ ) and required only 24 minutes to spend 75% in the warmer half, the TRPM8-deficient mice required 22 minutes to spend 50% of the subsequent test time above  $27.5^{\circ}\text{C}$  and after that they never located to more than 73% of the experimental time in the warmer semicircle (Fig. 3D).

Surprisingly, this evident phenotype vanished almost entirely when we measured the TRPM8-deficient mice in the larger 12-zone assay. Here, the mice located to a preference temperature of  $32.5^{\circ} \pm 2.4^{\circ}\text{C}$  after 45 mins, which was merely different from controls which preferred  $33.3^{\circ} \pm 3.1^{\circ}\text{C}$  ( $p=0.4$ , ANOVA, Table 2). Much in contrast to the small assay, they also showed almost no avoidance of warmer zones during exploratory behavior and the time until they spend at least 50% and 75% in the warmer semicircle was just like controls, 11 (8) and 25 (25) minutes, respectively (Fig. 4A, D). Thus, both phenotypes, warm avoidance and decreased cold avoidance, are much reduced in the larger assay. Some behavioral

differences became apparent when the time course was calculated for zones with temperature higher than  $32^{\circ}\text{C}$ , because the TRPM8-deficient mice spent less than 60% of the second half hour of the experiment above  $32^{\circ}\text{C}$  (33%), while the C57BL/6J spent more than 70% of the time above  $32^{\circ}\text{C}$  (Fig. 4C).

#### **Additional lack of TRPA1 decreases cold avoidance in TRPM8-deficient mice**

We next analyzed the behavior of TRPA1 knockouts and of TRPM8/A1 double knockouts in the gradient assay. While TRPA1-deficient mice did not differ from C57BL/6J mice in their overall preference temperature ( $33.1 \pm 2.5^{\circ}\text{C}$ ;  $p = 0.9$ , ANOVA, Table 2), we found that they were markedly faster in recognizing warmer zones as preferable. This is illustrated in the histogram view (Fig. 4A) and additionally reflected in the time course of thermal selection, where the TRPA1<sup>-/-</sup> required only 14 minutes to spend more than 50% of the time above  $32^{\circ}\text{C}$  – in contrast to 28–30 min for wildtype littermates or TRPM8-deficient mice, respectively (Fig. 4C). As for the phenotype of the double knockout mice, we found that lack of TRPA1- in TRPM8-knockouts reduces cold avoidance markedly. The phenotype of the double knockout mice was previously assessed in a 2-plate choice assay and found to be not different from single TRPM8<sup>-/-</sup> mice.<sup>12</sup> In our assembly the double knockout mice displayed a prominent reduction in cold avoidance behavior in the 12 zone assay, locating to  $29.8^{\circ} \pm 3.6^{\circ}\text{C}$ , at  $3.5^{\circ}\text{C}$  colder temperatures than controls ( $p = 0.0003$ , ANOVA) and  $2.7^{\circ}\text{C}$  lower than TRPM8<sup>-/-</sup> ( $p = 0.005$ , ANOVA). This behavior is especially apparent in the last 15 min of test time (Fig. 4B; Table 2). The thermal selection time course for  $>32^{\circ}\text{C}$  further illustrates this finding and shows that TRPM8/A1-deficient mice locate to these thermal zones randomly (33% likelihood throughout the experiment) (Fig. 4C). Nevertheless, the time lag until they spend at least 50% above  $27.5^{\circ}\text{C}$  was 12 min and similar to the TRPM8<sup>-/-</sup>; but the double knockout mice never

**Table 1.** Values of preference temperature and SD in the 8 zone assay.

Bins Descriptor Strain	1–15 mins		15–30 mins		30–45 mins		45–60 mins	
	Pref. Temp. ( $^{\circ}\text{C}$ )	SD	Pref. Temp. ( $^{\circ}\text{C}$ )	SD	Pref. Temp. ( $^{\circ}\text{C}$ )	SD	Pref. Temp. ( $^{\circ}\text{C}$ )	SD
WT (C57BL/6J)	$28.6 \pm 1.3$	7.4	$29.9 \pm 2.3$	6.0	$32.6 \pm 2.8$	4.2	$32.9 \pm 2.4$	3.4
TRPM8 <sup>-/-</sup>	$26.2 \pm 1.5$	7.2	$26.8 \pm 3.2$	6.6	$28.3 \pm 3.6$	5.9	$29.7 \pm 3.5$	5.2



**Table 2.** Comparison of the strains in the 12 zone assay.

Bins	Strains	Descriptors of distribution		
		Mean (°C) $\pm$ SD	SD	Skew
1–15 mins	WT (C57BL/6J)	27.6 $\pm$ 1.3	7.14	0.03
	TRPA1 <sup>-/-</sup>	28.7 $\pm$ 3.0	7.49	-0.16
	TRPM8 <sup>-/-</sup>	27.6 $\pm$ 1.7	7.03	0.03
	TRPM8/A1 <sup>-/-</sup>	26.6 $\pm$ 2.1	7.33	0.15
15–30 mins	WT (C57BL/6J)	29.6 $\pm$ 2.5	6.41	-0.49
	TRPA1 <sup>-/-</sup>	30.1 $\pm$ 3.7	6.83	-0.74
	TRPM8 <sup>-/-</sup>	29.3 $\pm$ 2.4	5.96	-0.56
	TRPM8/A1 <sup>-/-</sup>	27.7 $\pm$ 3.7	6.90	-0.23
30–45 mins	WT (C57BL/6J)	32.18 $\pm$ 3.2	5.35	-1.24
	TRPA1 <sup>-/-</sup>	32.1 $\pm$ 2.8	5.21	-1.37
	TRPM8 <sup>-/-</sup>	31.1 $\pm$ 3.4	4.80	-1.02
	TRPM8/A1 <sup>-/-</sup>	29.2 $\pm$ 3.9	6.02	-0.65
45–60 mins	WT (C57BL/6J)	33.3 $\pm$ 3.1	4.34	-1.91
	TRPA1 <sup>-/-</sup>	33.2 $\pm$ 2.5	4.35	-1.90
	TRPM8 <sup>-/-</sup>	32.5 $\pm$ 2.4	3.65	-1.26
	TRPM8/A1 <sup>-/-</sup>	29.8 $\pm$ 3.6	5.10	-0.68

spend more than 75% of their time above 27.5°C (Fig. 4D). Most remarkably, the double knockout mice still select warmer floor temperatures and show a similar standard deviation in comparison to C57BL/6J, TRPA1<sup>-/-</sup> and TRPM8<sup>-/-</sup>, although they locate to significantly lower temperatures than all other strains (Fig. 4B). This finding confirms in principle our previous finding of a contribution of TRPA1 to innocuous temperature sensing.<sup>18</sup>

### Skew measures another aspect of thermal selection behavior

Skew is calculated from the third power of the data. It expresses how asymmetric values are distributed about the mean. With a normal distribution, the skew  $\gamma$  is zero which signifies that mice would spend equal amounts of time above and below  $\mu$ , the arithmetic preference temperature;  $\gamma$  becomes positive if a tail extends to the right and negatively skew data have a negative  $\gamma$  and a tail to the left. Thus, in this experiment, positively skew data may in general be an indicator of a preference of colder temperatures and negatively skew data of a preference of warmer temperatures, respectively; albeit it must be kept in mind that skew is a parameter that is derived from the distribution about the mean preference temperature at each considered time point and does not directly refer to the median temperature in the ring. Thus in a case where e.g., several cold zones are entirely avoided by all individuals and the data are symmetrically distributed about the mean, the skew becomes zero although mice are only occupying the warmer half of the ring

(Fig. 5). In addition, skew cannot be calculated when only one zone is covered, because SD results as zero. Taken together, in this experiment, skew's explanatory power increases with the measured N and when it is calculated over a distribution that covers a sufficiently long timeframe (Fig. 5, Table 2). If these aspects are kept in mind, skew may be an important parameter to detect changes in thermal selection where preference temperature and SD hold statistically indifferent values, but show statistically different distribution of values about the mean. This was seen for TRPM8<sup>-/-</sup> in the 12 zone assay in the last 15 min of the experiment where TRPM8<sup>-/-</sup> show a broader distribution about the mean than wildtype mice (Fig. 4A). This distribution yields less negative skew (Table 2). The scatterplot in Figure 5A gives skew in 5 min resolution and illustrates a separation for TRPM8<sup>-/-</sup> (range 0.09; -1.27) and TRPM8/A1<sup>-/-</sup> (range 0.32; -0.79) vs. WT (range 0.18; -1.86) and TRPA1<sup>-/-</sup> (range -0.01; -1.95) and shows how skew changes over time alongside with the changing thermal selection of the animals (Fig. 5A). Interestingly the double knockouts show least left-skew distributions due to more symmetric distribution about the mean. This appears alongside with lower and a reduced range of preferred temperatures (Fig. 5B). Because reduced upper and lower bounds directly affect skew, we related time course of skew in minute resolution with zone occupancy in TRPM8 and TRPM8/A1-knockout mice. Figure 5C illustrates how altered lower and upper bounds of the distribution lead to less negative values for skew in TRPM8<sup>-/-</sup> between mins 38-41 and 50-52, where all measured individuals avoided the colder zones. In contrast, for TRPM8/A1<sup>-/-</sup>, which cover a reduced range of preferred temperatures, the less negative values of skew are not the result of reduced upper or lower bounds. For each calculated skew value, TRPM8/A1<sup>-/-</sup> covered all zones of the assay (Fig. 5C). This finding illustrates the need to relate skew to the respective data bounds.

### Discussion

Temperature-based assays for mouse models are widely used to assess the contribution of various ion channels to cold sensing and nociception and for algescic and analgesic drug screening. Assessing a subjective and highly variable phenomenon such as pain and aversion to innocuous temperature in mice, which

are more erratic in behavioral responses and less well conditionable than rats, represents a challenge *per se*. In fact given the circumstance that many of the described commonly used assays depend on accuracy and attention of one observer and therefore are prone to conscious and unconscious bias, any single disparity in experimental condition can affect data reproducibility and result in misinterpretations. Some of the challenge can be met by appropriate blinding and randomization of the experiment, but standardization of experiments and elimination of experimenter bias by computer-based analysis of behavioral data is

superior and meanwhile an emerging trend.<sup>7,25-27</sup> In that sense, our improved design of a thermal preference screening device with automated analysis, where values are assessed in duplicate and repulsing or attracting effects of corners are eliminated, yielded novel unrecognized characteristics of TRPM8-, TRPA1- and the double knockout mice. The circular design allows accurate measurement of zone distribution and enables to derive skew as valuable parameter to describe thermal selection behavior.

In mice, in contrast to primates, cold sensing is a feature of C-fibers, rather than A $\delta$ -fibers.

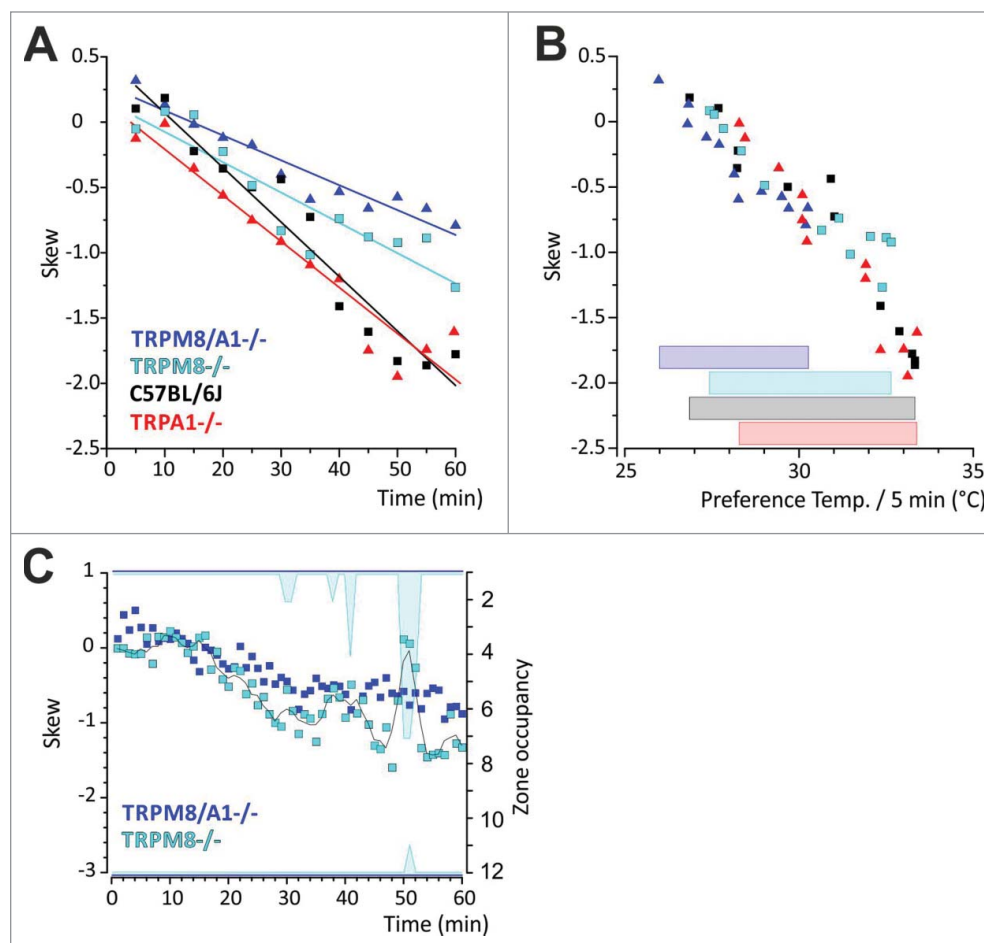


**Figure 5.** Skew as parameter to describe thermal preference behavior. (A) Linear regression analysis of skew and time. Skew is given as average per 5 mins. (A) In contrast to controls and TRPA1<sup>-/-</sup>, histogram distribution of thermal preference behavior of TRPM8 and TRPM8/A1-deficient mice yield less negative values for skew resulting from a less left-tailed distribution and corresponding to a preference of colder floor temperatures. (B) Scatterplot of skew and preference temperature in 5 min bins. Reduced range of preferred temperatures and colder preference temperatures in TRPM8/A1<sup>-/-</sup> correspond to less negatively skew data. Specifically, the bars at the bottom of the panel illustrate the range of preference temperature for each strain, C57BL/6J (black), TRPA1<sup>-/-</sup> (red), TRPM8<sup>-/-</sup> (cyan) and TRPM8/A1<sup>-/-</sup> (blue); (C) Influence of altered upper or lower bounds on skew. Skew is calculated in minute resolution for TRPM8<sup>-/-</sup> and TRPM8/A1<sup>-/-</sup>. Right y-axis illustrates zone occupancy in each minute. Cyan areas indicate zones that were left uncovered. In TRPM8<sup>-/-</sup> upper or lower bounds are reduced in mins 30–31, 38–41 and 50–52 which is the result for reduced values for skew. Black line is 3pt average. TRPM8/A1<sup>-/-</sup> show left tailed skews with progressive change over time due to thermal selection with bounds unchanged.

Thermoreceptors are characterized by a range of temperature thresholds between 37°C and 15°C. They exhibit fast adaptation characteristics to dynamic stimuli in the innocuous cool range and static coding properties within the dynamic range.<sup>28-31</sup> TRPM8 has been described as the principal cold sensor on cold nociceptors (CMC) and on thermoreceptors (CC). CMC fibers are absent in TRPM8<sup>-/-</sup>, while CC fiber classes suffer significant coding deficits.<sup>32,33</sup> This underlies the overt deficits of TRPM8<sup>-/-</sup> knockout animals to perceive cool between 10 and 25°C as assessed by 3 different authors when they challenged the animals in different settings.<sup>5-7</sup> While Colburn and Bautista tested thermal selection in a 2-temperature plate assay for 3 and 5 mins respectively, the plate sizes used by Colburn were roughly 3 times as large (20\*20 cm) as those used by Bautista which were hardly larger than the size of the mouse itself. In the case of a choice between a 5°C versus a 30°C surface this made an apparent difference and mice on the larger surfaces spent similar times on both surfaces whereas mice on the smaller surfaces were deterred by the 5°C like the wildtype littermates. Differentials in the innocuous range between 15 and 25 were recognized similar by both plate sizes assuming that either short measurement time increases uncertainty or that plate size may represent an essential experimental parameter under certain conditions. Dhaka extended measurement time in a large plate configuration (25\*10 cm) to 30 mins with the conclusion that avoidance to noxious cold temperatures (10°C) is not extinguished in TRPM8<sup>-/-</sup> and that lack of innocuous cold avoidance (18–31°C) it is not a matter of an abbreviated acquisition time, although in the second 15 minute bin, his TRPM8<sup>-/-</sup> showed increased, but still reduced preference for the warmer surface as compared to the first bin. This trend was reproduced in our measurements and present in both rings. It signifies that TRPM8-deficient mice can discern innocuous cold temperatures but require more time – in our small ring at least 30 mins; maybe warm sensing pathways which become activated every time when the mice cross the 40°C fields may partly direct the orientation. In fact, in TRPM8<sup>-/-</sup> warm temperatures may be perceived as more intense, because of the relative overweight of CMW and CMH fibers with low temperature thresholds identified in skin-nerve preparations of TRPM8<sup>-/-</sup>.<sup>32</sup> This may be a reason for the increased avoidance of warm areas in the smaller

assay; however it does not explain why this phenomenon is not present or compensated in the large ring.

In fact of particular interest appears the disparity that TRPM8-deficient mice manifested much larger cold sensing deficits in the smaller ring with the 0.47°C/cm gradient as to the larger ring with the 0.31°C/cm gradient. In contrast thermal selection behavior in C57BL/6J mice was independent of the size of the tempered surface or the slope of the gradient, 0.31°C/cm and 0.47°C/cm. Dhaka were the first to describe a preference analysis of the TRPM8<sup>-/-</sup>, but they used a temperature preference assay with linear design and a 0.39°C/cm gradient and inclusion of noxious hot temperatures. They assessed data during 90 mins in 3 30 min bins using a mouse tracking software based on a 20 zone resolution with 1.5°C differential between virtual adjacent zones. In contrast to our findings, their assessment yielded no thermal preference in the first 30 min of observation with a weighted preference temperature of ~22°C in TRPM8<sup>-/-</sup>. Their measurements were influenced by the general presence of a 15°C corner preference zone, a confounder which is eliminated by our design. TRPM8-deficient mice showed thermal selection in the small ring in terms of a clear avoidance of warmer areas in the small ring in the first 30 min bin, while in the large ring thermal selection was similar to the wildtype animals. After 90 min, Dhaka determined the preference of wildtype mice to a range of warm temperatures between 30–38°C (weighted average of 32°C). The TRPM8<sup>-/-</sup> had a wider range of preference temperatures between 23–38°C and with a weighted average of 28°C after 90 mins. In our device, C57BL/6J mice located already after 60 mins to a much narrower range of temperatures between 31.2–34.6°C in the small ring and to 31.2–35.4°C in the large ring - this represents a clear advantage of our ring-shaped design. For TRPM8<sup>-/-</sup> this was significantly lower especially for the 3rd and 4th bin in the small ring with the mice choosing temperatures between 26.4–33°C in the 4th bin, in contrast to 30.2–34.8°C in the large ring.

As evident from our data in [Figures 3 and 4](#), we assume that the overall size of the ring surface is probably less important for the observed differences in perception of the TRPM8<sup>-/-</sup> in both ring shapes; probably unless a certain size limit is not underrun where the device is so small that it resembles a 2 plate configuration with high differential. We also assume

that the ring-shape of the device with duplicate measurement and elimination of edge artifacts preferentially increases accuracy of the results and potentially reduces the measurement time, because we achieved a reduction in SD at earlier timepoints than others in the linear-shaped device.<sup>7,34,35</sup> We speculate that the key aspect mediating the different finding of thermal preference in both assays may relate to the steeper temperature gradient in the smaller ring and a function of TRPM8 as differential cold sensor in the cool/cold temperature range.

Differential sensitivity to cold is a feature of the CC-fibers<sup>30,32</sup> which are lacking in TRPM8<sup>-/-</sup>.<sup>33</sup> The lack of these fibers may result in imbalance of input from cold and warm fibers and for some reason may be better compensated for when gradients are less steep which also entails a reduced warm aversive behavior in the large ring. In fact, the critical area for the measured preferendum between 26–33°C is in the smaller gradient about 13.4 cm long compared to the larger assay with about 20 cm. Assuming average mouse length during common explorative behavior approximately 7 cm, the steep temperature gradient in the small ring causes a relatively large temperature difference between mouse fore- and hind paw and might confront the animal with a perception mismatch and difficulty in finding its exact optimal temperature spot. This may provoke a more erratic behavior and lead it to withdraw to more “safer” zones, away from potential harm due to intense warm or suspected excessive heat.

Warm fibers, however, are presumably not the only factor guiding the thermal choice in TRPM8-deficient mice, because increasing warm preference of TRPM8<sup>-/-</sup> mice in later timepoints of the 2 temperature preference assay was also observed in 10–14°C and in 26–30°C differentials,<sup>7</sup> thus temperatures below the reported activation threshold of warm fibers. This behavior, and potentially the absence of warm avoidance in the larger assay, implies the presence of other mechanism(s) of cold sensing and therefore the large assay represented for us the assay format for further investigations with TRPA1-deficient mice.

Surprisingly, TRPA1 knock-out animals migrated more rapidly to the warmer zones in the 2nd bin (Fig. 4A and C) and had the same preference behavior as wildtype mice in the 4th bin. TRPA1<sup>-/-</sup> had also more negatively skew data during the first 45 mins of the experiment than C57BL/6J (Fig. 5A, Table 2).

Nevertheless accumulating evidence especially from nociceptive assays, including cold plate and tail withdrawal, and from fMRI recordings, strongly support the assumption of TRPA1 being implicated in cold temperature detection.<sup>13,14,16,18,36,37</sup> In contrast to these assays our paradigm measures a complex behavioral response pattern over a longer timeframe. One possible and simple explanation is that cold-activated TRPA1-carrying pathways exert inhibition on warm or heat-sensing pathways at the level of the spinal cord or the brain - similar to the tonic cross inhibition of cold sensing pathways unveiled for CGRP-carrying fibers.<sup>38</sup> Disruption of crosstalk would unmask in TRPA1<sup>-/-</sup> a disinhibition of warm-sensing fibers which may then indeed result in faster warm temperature recognition and speeded thermal selection behavior. If this is the case, it may in part account for the difficulty to assess the contribution of TRPA1 to cold sensing encountered in the past with other assays which generated a series of conflicting results. Certainly, alternative explanations exist and may have to do with the complex behavior of the channel and the thermodynamic prediction that cold-sensing TRPs are also hot-sensing.<sup>39</sup> Nevertheless, additional lack of TRPM8 in TRPA1<sup>-/-</sup> revealed a major contribution of TRPA1 to innocuous cold temperature perception, because double knockout mice showed a largely augmented reduction of cold aversive behavior. Obviously the contribution of TRPA1 to innocuous cold temperature sensing exists and it is important, but in TRPA1<sup>-/-</sup> it is to large parts compensated for by a functional TRPM8. Our findings contrast with a previous report where these mice were assessed in a 2-plate temperature choice assay and where no difference to TRPM8<sup>-/-</sup> became obvious.<sup>12</sup> Our result speaks for an increased sensitivity of the gradient assay in comparison to 2-plate choice configurations in this temperature range. Seemingly, TRPA1s contribution to cold sensing is more complicated than assumed and our results may also indicate that TRPA1 functions as TRPM8-associated or TRPM8-dependent signal enhancer or holds another indirect function that depends or is facilitated by the simultaneous activation of TRPM8 or other TRPM8-dependent channels or proteins. Nevertheless this result is in line with our previous finding of a general reduction in BOLD signal in an fMRI experiment with TRPA1<sup>-/-</sup> in response to stimulation of the paw with temperatures in the 15°C range. While an involvement of TRPA1 in

noxious cold sensing became apparent in several tests, in the gradient assay a deficit in the innocuous temperature range became only apparent when a second cold transduction mechanism failed. Interestingly, several studies show that TRPA1 is not coexpressed on the same neuronal subpopulation as TRPM8<sup>10,17</sup> so the precise mechanism of how TRPA1 influences the temperature perception in TRPM8-deficient mice remains to be clarified, but may also lie in the spinal cord where different cold sensing pathways converge and enter into circuits at the postsynaptic level in the superficial laminae of the spinal cord where they undergo cross-inhibition by pathways of other modalities.<sup>38</sup> Also other factors, including changes in body temperature and thermoregulatory behavior may come into effect with longer measurement times.

Testing temperature sensitivity is the modality of choice for many studies addressing fundamental aspects of nociception and pain signaling. Future evaluations will determine whether results from thermal gradient assay in combination with neuropathic pain, inflammatory pain or pharmacologic models of cold allodynia<sup>40,41</sup> correlate with results from acute nociception tests that measure primary afferent processes and spinal nociceptive reflexes like the tail-flick test, hot and cold plate test and the Hargreaves test. In comparison to these assays the thermal gradient paradigm is more complex; it involves integration of primary afferent information and spinal cord and brain processes of temperature perception and autonomic and behavioral thermoregulation. Nevertheless our assay clearly provides superior accuracy than a simple linear gradient design and any 2-plate choice configuration. In the literature results from the latter is frequently assumed to reflect the animal's general temperature preference although measurements are often only assessed during 5 mins or less, because these assays are manpower intensive, even when they are automated, and require multiple trials at each temperature to extract full temperature response relationships.

## Abbreviations

A $\delta$ -fibers	Group A delta nerve fiber
ANOVA	analysis of variance
BOLD	Blood Oxygenation Level Dependent
CC	Group C cold thermoreceptor
CCD	camera charged-coupled device camera
C-fibers	Group C nerve fiber
CMC	Group C mechano cold nociceptor
fMRI	functional Magnetic Resonance Imaging

LSD	least significant difference
QC	quality control
SD	standard deviation
SEM	standard error of the mean
TRP	Transient Receptor Potential
TRPA1	Transient Receptor Potential Ankyrin 1 receptor
TRPM8	Transient Receptor Potential Melastatin 8 receptor

## Disclosure of potential conflicts of interest

No potential conflicts of interest were disclosed.

## Acknowledgments

We would like to thank the “Sonderfonds für wissenschaftliche Arbeiten an der Universität Erlangen-Nürnberg” for sponsoring the infrared camera used in this study. Jana Schramm performed expert technical assistance. We thank Harald Ihmsen (Department of Anesthesiology, Universitätsklinikum der Friedrich-Alexander Universität, Erlangen, Germany) for insightful comments on the manuscript and Jeffrey Mogil (Pain Genetics Lab, McGill-University, Montreal, Canada) for provoking this approach to data analysis.

## Funding

Funding for this project was obtained through the German Research Council (DFG): Zi1172/2-1, Zi1172/3-1 and Zi1172/4-1 (KZ); IZKF project E14 (KZ); the Czech Science Foundation (GACR) 15-15839S (FT, VV).

## References

- [1] Vriens J, Nilius B, Voets T. Peripheral thermosensation in mammals. *Nat Rev Neurosci* 2014; 15:573-89; PMID:25053448; <http://dx.doi.org/10.1038/nrn3784>
- [2] Romanovsky AA. Skin temperature: its role in thermoregulation. *Acta Physiol (Oxf)* 2014; 210:498-507; PMID:24716231; <http://dx.doi.org/10.1111/apha.12231>
- [3] Peier AM, Moqrich A, Hergarden AC, Reeve AJ, Andersson DA, Story GM, Earley TJ, Dragoni I, McIntyre P, Bevan S, et al. A TRP channel that senses cold stimuli and menthol. *Cell* 2002; 108:705-15; PMID:11893340; [http://dx.doi.org/10.1016/S0092-8674\(02\)00652-9](http://dx.doi.org/10.1016/S0092-8674(02)00652-9)
- [4] McKemy DD, Neuhauser WM, Julius D. Identification of a cold receptor reveals a general role for TRP channels in thermosensation. *Nature* 2002; 416:52-8; PMID:11882888; <http://dx.doi.org/10.1038/nature719>
- [5] Colburn RW, Lubin ML, Stone DJ Jr, Wang Y, Lawrence D, D'Andrea MR, Brandt MR, Liu Y, Flores CM, Qin N. Attenuated cold sensitivity in TRPM8 null mice. *Neuron* 2007; 54:379-86; PMID:17481392; <http://dx.doi.org/10.1016/j.neuron.2007.04.017>
- [6] Bautista DM, Siemens J, Glazer JM, Tsuruda PR, Basbaum AI, Stucky CL, Jordt SE, Julius D. The menthol receptor TRPM8 is the principal detector of environmental cold. *Nature* 2007; 448:204-8; PMID:17538622; <http://dx.doi.org/10.1038/nature05910>

- [7] Dhaka A, Murray AN, Mathur J, Earley TJ, Petrus MJ, Patapoutian A. TRPM8 is required for cold sensation in mice. *Neuron* 2007; 54:371-8; PMID:17481391; <http://dx.doi.org/10.1016/j.neuron.2007.02.024>
- [8] Bandell M, Story GM, Hwang SW, Viswanath V, Eid SR, Petrus MJ, Earley TJ, Patapoutian A. Noxious cold ion channel TRPA1 is activated by pungent compounds and bradykinin. *Neuron* 2004; 41:849-57; PMID:15046718; [http://dx.doi.org/10.1016/S0896-6273\(04\)00150-3](http://dx.doi.org/10.1016/S0896-6273(04)00150-3)
- [9] Bautista DM, Jordt SE, Nikai T, Tsuruda PR, Read AJ, Poblete J, Yamoah EN, Basbaum AI, Julius D. TRPA1 mediates the inflammatory actions of environmental irritants and proalgesic agents. *Cell* 2006; 124:1269-82; PMID:16564016; <http://dx.doi.org/10.1016/j.cell.2006.02.023>
- [10] Story GM, Peier AM, Reeve AJ, Eid SR, Mosbacher J, Hricik TR, Earley TJ, Hergarden AC, Andersson DA, Hwang SW, et al. ANKTM1, a TRP-like channel expressed in nociceptive neurons, is activated by cold temperatures. *Cell* 2003; 112:819-29; PMID:12654248; [http://dx.doi.org/10.1016/S0092-8674\(03\)00158-2](http://dx.doi.org/10.1016/S0092-8674(03)00158-2)
- [11] Moparthy L, Survery S, Kreir M, Simonsen C, Kjellbom P, Högestätt ED, Johanson U, Zygmunt PM. Human TRPA1 is intrinsically cold- and chemosensitive with and without its N-terminal ankyrin repeat domain. *Proc Natl Acad Sci U S A* 2014; 111:16901-6; PMID:25389312; <http://dx.doi.org/10.1073/pnas.1412689111>
- [12] Knowlton WM, Bifolck-Fisher A, Bautista DM, McKemy DD. TRPM8, but not TRPA1, is required for neural and behavioral responses to acute noxious cold temperatures and cold-mimetics in vivo. *Pain* 2010; 150:340-50; PMID:20542379; <http://dx.doi.org/10.1016/j.pain.2010.05.021>
- [13] del Camino D, Murphy S, Heiry M, Barrett LB, Earley TJ, Cook CA, Petrus MJ, Zhao M, D'Amours M, Deering N, et al. TRPA1 contributes to cold hypersensitivity. *J Neurosci* 2010; 30:15165-74; PMID:21068322; <http://dx.doi.org/10.1523/JNEUROSCI.2580-10.2010>
- [14] Obata K, Katsura H, Mizushima T, Yamanaka H, Kobayashi K, Dai Y, Fukuoka T, Tokunaga A, Tominaga M, Noguchi K. TRPA1 induced in sensory neurons contributes to cold hyperalgesia after inflammation and nerve injury. *J Clin Invest* 2005; 115:2393-401; PMID:16110328; <http://dx.doi.org/10.1172/JCI25437>
- [15] Kwan KY, Allchorne AJ, Vollrath MA, Christensen AP, Zhang DS, Woolf CJ, Corey DP. TRPA1 contributes to cold, mechanical, and chemical Nociception but is not essential for hair-cell transduction. *Neuron* 2006; 50:277-89; PMID:16630838; <http://dx.doi.org/10.1016/j.neuron.2006.03.042>
- [16] Karashima Y, Talavera K, Everaerts W, Janssens A, Kwan KY, Vennekens R, Nilius B, Voets T. TRPA1 acts as a cold sensor in vitro and in vivo. *Proc Natl Acad Sci U S A* 2009; 106:1273-8; PMID:19144922; <http://dx.doi.org/10.1073/pnas.0808487106>
- [17] Pogorzala LA, Mishra SK, Hoon MA. The cellular code for mammalian thermosensation. *J Neurosci* 2013; 33:5533-41; PMID:23536068; <http://dx.doi.org/10.1523/JNEUROSCI.5788-12.2013>
- [18] Vetter I, Touska F, Hess A, Hinsbey R, Sattler S, Lampert A, Sergejeva M, Sharov A, Collins LS, Eberhardt M, et al. Ciguatoxins activate specific cold pain pathways to elicit burning pain from cooling. *EMBO J* 2012; 31:3795-808; PMID:22850668; <http://dx.doi.org/10.1038/emboj.2012.207>
- [19] Carlisle HJ, Frost TS, Stock MJ. Thermal preference behavior following clonidine, norepinephrine, isoproterenol, and ephedrine. *Physiol Behav* 1999; 66:585-9; PMID:10386901; [http://dx.doi.org/10.1016/S0031-9384\(98\)00328-X](http://dx.doi.org/10.1016/S0031-9384(98)00328-X)
- [20] Refinetti R, Carlisle HJ. Effects of lateral hypothalamic lesions on thermoregulation in the rat. *Physiol Behav* 1986; 38:219-28; PMID:3797489; [http://dx.doi.org/10.1016/0031-9384\(86\)90157-5](http://dx.doi.org/10.1016/0031-9384(86)90157-5)
- [21] Gordon CJ. Twenty-four-hour control of body temperature in rats. I. Integration of behavioral and autonomic effectors. *Am J Physiol* 1994; 267:R71-77; PMID:8048648
- [22] Gordon CJ, Becker P, Killough P, Padnos B. Behavioral determination of the preferred foot pad temperature of the mouse. *J Therm Biol* 2000; 25:211-9; [http://dx.doi.org/10.1016/S0306-4565\(99\)00025-X](http://dx.doi.org/10.1016/S0306-4565(99)00025-X)
- [23] Gordon CJ, Kimm-Brinson KL, Padnos B, Ramsdell JS. Acute and delayed thermoregulatory response of mice exposed to brevetoxin. *Toxicol* 2001; 39:1367-74; PMID:11384725; [http://dx.doi.org/10.1016/S0041-0101\(01\)00092-7](http://dx.doi.org/10.1016/S0041-0101(01)00092-7)
- [24] Vetter I, Hein A, Sattler S, Hessler S, Touska F, Bressan E, Parra A, Hager U, Leffler A, Boukalova S, et al. Amplified cold transduction in native nociceptors by M-channel inhibition. *J Neurosci* 2013; 33:16627-41; PMID:24133266; <http://dx.doi.org/10.1523/JNEUROSCI.1473-13.2013>
- [25] Knowlton WM, Palkar R, Lippoldt EK, McCoy DD, Baluch F, Chen J, McKemy DD. A sensory-labeled line for cold: TRPM8-expressing sensory neurons define the cellular basis for cold, cold pain, and cooling-mediated analgesia. *J Neurosci* 2013; 33:2837-48; PMID:23407943; <http://dx.doi.org/10.1523/JNEUROSCI.1943-12.2013>
- [26] Brodtkin J, Frank D, Grippo R, Hausfater M, Gulinello M, Achterholt N, Gutzen C. Validation and implementation of a novel high-throughput behavioral phenotyping instrument for mice. *J Neurosci Methods* 2014; 224:48-57.
- [27] Yin K, Zimmermann K, Vetter I, Lewis RJ. Therapeutic opportunities for targeting cold pain pathways. *Biochem Pharmacol* 2015; 93:125-40; PMID:25316567; <http://dx.doi.org/10.1016/j.bcp.2014.09.024>
- [28] Campero M, Serra J, Bostock H, Ochoa JL. Slowly conducting afferents activated by innocuous low temperature in human skin. *J Physiol* 2001; 535:855-65; PMID:11559780; <http://dx.doi.org/10.1111/j.1469-7793.2001.t01-1-00855.x>
- [29] Fujita F, Uchida K, Takaishi M, Sokabe T, Tominaga M. Ambient temperature affects the temperature threshold for TRPM8 activation through interaction of phosphatidylinositol 4,5-bisphosphate. *J Neurosci* 2013; 33:6154-9; PMID:23554496; <http://dx.doi.org/10.1523/JNEUROSCI.5672-12.2013>

- [30] Zimmermann K, Hein A, Hager U, Kaczmarek JS, Turnquist BP, Clapham DE, Reeh PW. Phenotyping sensory nerve endings in vitro in the mouse. *Nat Protoc* 2009; 4:174-96; PMID:19180088; <http://dx.doi.org/10.1038/nprot.2008.223>
- [31] Brenner DS, Golden JP, Vogt SK, Dhaka A, Story GM, Gereau Iv RW. A dynamic set point for thermal adaptation requires phospholipase C-mediated regulation of TRPM8 in vivo. *Pain* 2014; 155:2124-33; PMID:25109670; <http://dx.doi.org/10.1016/j.pain.2014.08.001>
- [32] Zimmermann K, Lennerz JK, Hein A, Link AS, Kaczmarek JS, Dellinger M, Uysal S, Pfeifer JD, Riccio A, Clapham DE. Transient receptor potential cation channel, subfamily C, member 5 (TRPC5) is a cold-transducer in the peripheral nervous system. *Proc Natl Acad Sci U S A* 2011; 108:18114-9; PMID:22025699; <http://dx.doi.org/10.1073/pnas.1115387108>
- [33] Toro CA, Eger S, Veliz L, Sotelo-Hitschfeld P, Cabezas D, Castro MA, Zimmermann K, Brauchi S. Agonist-dependent modulation of cell surface expression of the cold receptor TRPM8. *J Neurosci* 2015; 35:571-82; PMID:25589752; <http://dx.doi.org/10.1523/JNEUROSCI.3820-13.2015>
- [34] Lee HS, Iida T, Mizuno A, Suzuki M, Caterina MJ. Altered thermal selection behavior in mice lacking transient receptor potential vanilloid 4. *J Neurosci* 2005; 25:1304-10; PMID:15689568; <http://dx.doi.org/10.1523/JNEUROSCI.4745.04.2005>
- [35] Huang SM, Li X, Yu Y, Wang J, Caterina MJ. TRPV3 and TRPV4 ion channels are not major contributors to mouse heat sensation. *Mol Pain* 2011; 7:37; PMID:21586160; <http://dx.doi.org/10.1186/1744-8069-7-37>
- [36] Aubdool AA, Graepel R, Kodji X, Alawi KM, Bodkin JV, Srivastava S, Gentry C, Heads R, Grant AD, Fernandes ES, et al. TRPA1 is essential for the vascular response to environmental cold exposure. *Nat Commun* 2014; 5:5732.
- [37] Gentry C, Stoakley N, Andersson DA, Bevan S. The roles of iPLA2, TRPM8 and TRPA1 in chemically induced cold hypersensitivity. *Mol Pain* 2010; 6:4; PMID:20092626; <http://dx.doi.org/10.1186/1744-8069-6-4>
- [38] McCoy ES, Taylor-Blake B, Street SE, Pribisko AL, Zheng J, Zylka MJ. Peptidergic CGRP  $\alpha$  Primary Sensory Neurons Encode Heat and Itch and Tonicly Suppress Sensitivity to Cold. *Neuron* 2013; 78:138-51; PMID:23523592; <http://dx.doi.org/10.1016/j.neuron.2013.01.030>
- [39] Clapham DE, Miller C. A thermodynamic framework for understanding temperature sensing by transient receptor potential (TRP) channels. *Proc Natl Acad Sci U S A* 2011; 108:19492-7; PMID:22109551; <http://dx.doi.org/10.1073/pnas.1117485108>
- [40] Deuis JR, Zimmermann K, Romanovsky AA, Possani LD, Cabot PJ, Lewis RJ, Vetter I. An animal model of oxaliplatin-induced cold allodynia reveals a crucial role for Nav1.6 in peripheral pain pathways. *Pain* 2013; 154:1749-57; PMID:23711479; <http://dx.doi.org/10.1016/j.pain.2013.05.032>
- [41] Zimmermann K, Deuis JR, Inerra MC, Collins LS, Namer B, Cabot PJ, Reeh PW, Lewis RJ, Vetter I. Analgesic treatment of ciguatoxin-induced cold allodynia. *Pain* 2013; 154:1999-2006; PMID:23778293; <http://dx.doi.org/10.1016/j.pain.2013.06.015>